NeuroImage 86 (2014) 150–163

Contents lists available at ScienceDirect

NeuroImage

journal homepage: www.elsevier.com/locate/ynimg

A multivariate analysis of age-related differences in functional networks supporting conflict resolution

Alireza Salami [a,b,*], Anna Rieckmann [a], Håkan Fischer [c], Lars Bäckman [a]

[a] Aging Research Center, Karolinska Institutet, Stockholm, Sweden
[b] Umeå Center for Functional Brain Imaging, S-90187, Umeå, Sweden
[c] Department of Psychology, Stockholm University, Stockholm, Sweden

ARTICLE INFO

Article history:
Accepted 1 August 2013
Available online 9 August 2013

Keywords:
Aging
Interference resolution
MSIT
PLS
Reorganization
Functional connectivity

ABSTRACT

Functional neuroimaging studies demonstrate age-related differences in recruitment of a large-scale attentional network during interference resolution, especially within dorsolateral prefrontal cortex (DLPFC) and anterior cingulate cortex (ACC). These alterations in functional responses have been frequently observed despite equivalent task performance, suggesting age-related reallocation of neural resources, although direct evidence for a facilitating effect in aging is sparse. We used the multi-source interference task and multivariate partial-least-squares to investigate age-related differences in the neuronal signature of conflict resolution, and their behavioral implications in younger and older adults. There were interference-related increases in activity, involving fronto-parietal and basal ganglia networks that generalized across age. In addition an age-by-task interaction was observed within a distributed network, including DLPFC and ACC, with greater activity during interference in the old. Next, we combined brain–behavior and functional connectivity analyses to investigate whether compensatory brain changes were present in older adults, using DLPFC and ACC as regions of interest (i.e. seed regions). This analysis revealed two networks differentially related to performance across age groups. A structural analysis revealed age-related gray-matter losses in regions facilitating performance in the young, suggesting that functional reorganization may partly reflect structural alterations in aging. Collectively, these findings suggest that age-related structural changes contribute to reductions in the efficient recruitment of a youth-like interference network, which cascades into instantiation of a different network facilitating conflict resolution in elderly people.

Introduction

Humans have access to information that originates from available external stimuli or can be retrieved from stored experiences. However, prepotent but task-irrelevant information may interfere with relevant information and impair performance. The ability to ignore irrelevant information has been investigated in several paradigms, with participants responding to stimuli in the presence or absence of distracting items (Bush et al., 2003; Eriksen and Eriksen, 1974; Simon and Berbaum, 1990; Stroop, 1935). Each paradigm relies on different methods for inducing cognitive conflict (for review, see Nee et al., 2007). For instance, the Stroop effect represents cognitive interference produced by color incongruence between a word depicting a color with the color of the ink (i.e. stimulus conflict), whereas the Simon effect denotes cognitive interference through spatial incongruence between the target and response (i.e. response conflict). The type of conflict resolution targeted in this research declines with age. Elderly persons have fewer resources available during a task conflict to inhibit irrelevant information (Gazzaley et al., 2008; Madden et al., 2004). Imaging studies have linked age-related deficits in conflict resolution to alterations in the anterior control network that involves DLPFC (Langenecker et al., 2004; Thomsen et al., 2004) and dorsal ACC (Milham et al., 2002), as well as the posterior attention network, including superior parietal cortex (Schulte et al., 2009). For example, Langenecker and colleagues reported similar brain activation patterns for younger and older adults during a Stroop task, along with age-related over-recruitment in frontal regions. The authors suggested that greater frontal activity among elderly people promotes successful inhibition. By contrast, Milham et al. found that older adults exhibited reduced DLPFC activity and greater ACC activity compared to younger adults during interference. Reduced DLPFC activity may reflect age-related impairment in attentional control, whereas increased ACC activity may indicate heightened potential for error.

Complex cognitive processes, such as interference resolution, may not be localized to discrete brain regions such as ACC and DLPFC, but rather be mediated by interactions among a set of functionally related areas (McIntosh, 1999). Functional connectivity (Friston et al., 1993; McIntosh, 1999) is an approach to directly assess interactions among

* Corresponding author at: Karolinska Institutet, Aging Research Center, Gävlegatan 16, SE-113 30 Stockholm, Sweden. Fax: +46 8 690 6889.
E-mail address: alireza.salami@ki.se (A. Salami).

1053-8119/$ – see front matter © 2013 Published by Elsevier Inc.
http://dx.doi.org/10.1016/j.neuroimage.2013.08.002

network nodes for a specific cognitive process and their alterations in aging, which in turn might affect behavior (e.g. Clapp et al., 2011; Grady et al., 2010; Nagel et al., 2011). For example, Clapp and colleagues reported age-related working memory deficits for scenes during a delayed matching-to-sample task along with disruption of functional connectivity between PFC and the parahippocampal place area. Despite increasing interest in understanding covarying activity within a network for determining the neural underpinnings of cognitive functions (Bressler and Menon, 2010; McIntosh, 1999), direct evidence regarding age-related differences in connectivity of critical nodes for conflict resolution (i.e., ACC, DLPFC) and concomitant behavioral implications is lacking. To date, few studies have reported how brain responses during interference are modulated by performance (Zysset et al., 2007), and no study has examined whole-brain patterns of activity in relation to performance (for review, see Grady, 2012). Similarly, past research on this topic has examined regional effects of age on conflict resolution and not reported data at the network level. Thus, although past research suggests age-related differences in functional activation of critical nodes for conflict resolution, they do not provide direct evidence as to whether unique brain networks promote interference resolution across different age groups.

In the context of possible functional alterations in aging, an important question is how age-related functional alterations relate to other factors that are also affected by aging and influence brain function, such as brain structure. There is robust evidence for age-related decline in brain volumes, particularly in the frontal lobes (Good et al., 2001; Raz et al., 2005). Age-related differences in gray-matter (GM) volume may locally account for regional alterations in functional responses (e.g. Kalpouzos et al., 2011; Salami et al., 2012). However, an examination of the full set of brain regions also reflecting potential distal associations is lacking (e.g. Calhoun et al., 2006; Stevens et al., 2009).

To assess age differences in conflict resolution and associated brain systems, multivariate spatial–temporal partial-least-squares (PLS; McIntosh et al., 1996, 2004) was applied to data from younger and older adults. Participants were scanned with functional magnetic resonance imaging (fMRI) while they performed the Multi-Source Interference Task (MSIT; Bush and Shin, 2006; Bush et al., 2003), which involves control and interference trials and the critical contrast concerns differences in accuracy and/or response latency between the two conditions. This task combines multiple dimensions of cognitive interference. Specifically, the MSIT contains elements of flanker interference (i.e. distracting items flanking the target; Eriksen and Eriksen, 1974) and Simon interference (i.e. incongruity between the position of the target and the position of the response; Simon and Berbaum, 1990). The MSIT engages the cingulo-fronto-parietal attentional network (Bush and Shin, 2006; Bush et al., 2003). To identify whole-brain activity during the two MSIT conditions for each age group, we initially applied task PLS analysis. As opposed to traditional analysis which largely rests on cognitive subtraction, PLS is able to use all conditions in an experiment at once, and thus provides an additional dimension to data by simultaneously considering indices of both similarities and differences across all grouping/experimental variables. If young and older adults engage many similar brain regions differentiating the two task conditions, task PLS analysis reveals an age-common network. Alternatively and/or in addition, if some brain regions exhibit age-differential activation between conditions, PLS analysis reveals group-specific networks. Another way in which interference resolution might be compromised in aging is that regions supporting interference resolution may remain relatively similar, although the functional connectivity within the network is altered. On this view, less proficient interference resolution in elderly people may be related to less efficient recruitment of the network promoting interference resolution in the young. Specifically, interference resolution might be compromised in older adults due to less efficient interaction within the anterior control network or the posterior attention network. Using seed PLS, we first examined whether functional connectivity among those network nodes reflecting the most reliable group differences varied between age groups and was modulated by performance. If younger and older adults alike engage the same network to support performance, the seed PLS should reveal a common circuitry with possible quantitative differences across age. Alternatively, if younger and older persons recruit distinct networks to support performance, the seed PLS should reveal networks differentially correlated with performance across age. This analysis allows us to verify whether the functional network supporting interference resolution in old age is similar to that recruited by the young, or constitutes a different network that may not facilitate interference resolution in younger adults. Finally, relationships between brain activity and GM volume were explored to investigate whether age-related differences in structural integrity are associated with age-related alterations in functional networks during interference resolution.

Methods

Participants

29 young (20–31 years of age, 16 females) and 29 old (65–74 years of age, 16 females) participants from Stockholm, Sweden participated. There were no significant age differences in years of education (Young: 14.7 ± 2.1; Old: 14.3 ± 3.7) or on a test of mental status (Mini Mental Status Examination, Folstein et al., 1975) (Young: 29.2 ± 0.7; Old: 28.9 ± 0.8). From the initial sample of 58 participants, four (three old, one young) were excluded due to low task performance (below chance level). Two older subjects were excluded due to not performing the task at all. Finally, one young subject was excluded due to technical error. All remaining participants (27 young and 24 old) were right-handed, native Swedish-speakers, had normal or corrected to normal vision, and had no history of neurological illness. In addition, participants neither reported nor were diagnosed with cognitive impairment (e.g. dementia, mild cognitive impairment). The ethics committee at the Karolinska Institute approved the protocol; informed consent was obtained from all participants.

fMRI activation task

The MSIT (Bush et al., 2003) consists of a total of 16 blocks of control and interference trials, alternating during the scanning session. Within each control and interference block (8 each), 12 stimuli were presented for 2 s each. Participants were given a button-press and instructed that the keypad buttons represented one, two, and three from left to right (Fig. 1A). They were informed that sets of three numbers (1 and/or 2 and/or 3) and/or the distracter number (0) would appear in the center of the screen and that one number would always be different from the other two numbers. During the control task, distracters were always the number zero, and the target number (1 or 2 or 3) was always placed congruently with its position on the button press (e.g. the number 3 always appeared at the rightmost position). In contrast, during the interference task, distracters were other numbers (1 or 2 or 3), and the target never matched its spatial position. Participants were asked to report the identity of the number that was different from the other two numbers, regardless of its position. They were also instructed to respond as accurately and quickly as possible (Fig. 1A).

Image acquisition

fMRI data were collected on a 3 T Siemens Magnetom TrioTim scanner at Huddinge Hospital, Stockholm, Sweden, with a 32-channel head coil. Scanner parameters for the gradient-echo EPI sequence were as follows: TR = 2.5 s, 39 slices (3.0 mm thick), voxel size 3 × 3 × 3 mm, FOV = 230 mm, flip angle = 90°, TE = 40 ms. Four dummy scans were collected to allow for equilibration of the fMRI signal. Stimuli

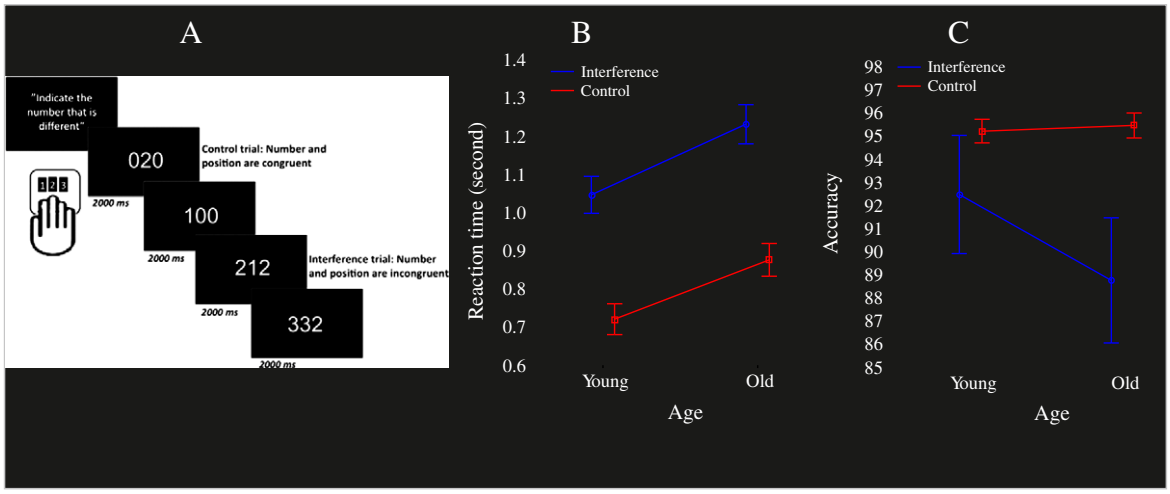

Fig. 1. The Multisource Interference Task (Bush et al., 2003) and behavioral results across the two age groups. (A) Participants are instructed to identify a digit that is different from two other digits, as fast and accurately as possible. Upon determining the unique target number, participants pressed the button corresponding to the correct response (the spatial location of the correct number) on a keypad with three buttons. (B) Reaction time during interference and control conditions across age groups. (C) Accuracy during interference and control conditions across age groups.

were presented on a computer screen that was seen by participants through a tilted mirror attached to the head coil. E-prime (Psychology Software Tools, Inc., Pittsburgh, USA; www.pstnet.com/eprime) was used for presentation of stimuli and responses were made on custom-built MR-compatible response pads (MAG Design & Engineering, Sunnyvale, California). Structural high-resolution T1-weighted images (200 slices, 1 mm thickness, FOV = 256 mm, voxel size = $1 \times 1 \times 1$ mm^3) were collected following the functional images.

Data analysis

Structural and functional data were preprocessed using statistical parametric mapping software (SPM8; Wellcome Department of Imaging Science, Functional Imaging Laboratory). All functional images were first corrected for differences in slice acquisition times within each volume using the middle slice as reference. The corrected images were then rigidly aligned to the first volume to correct for head movements. A within-subject rigid registration was carried out to align functional and structural images together, providing high resolution T1-weighted images for spatial normalization. T1-weighted images were segmented into gray matter (GM), white matter (WM), and cerebrospinal fluid (CSF) using a new segmentation algorithm in SPM8. Then, a group-specific template was created using diffeomorphic anatomical registration using exponentiated lie algebra (DARTEL; Ashburner, 2007). A detailed description for creating the template is provided elsewhere (Salami et al., 2012). Finally, the realigned fMRI images and the segmented GM/WM/CSF images were non-linearly normalized to the sample-specific group template, affine-aligned into MNI template, and smoothed using an 8.0-mm full-width at half-maximum Gaussian filter. Thus, both fMRI and GM/WM/CSF images were in the same space and had the same voxel size ($1 \times 1 \times 1$ mm).

The preprocessed fMRI image data were analyzed with spatiotemporal Partial-Least-Squares (PLS; McIntosh and Lobaugh, 2004; McIntosh et al., 2004) to assess commonalities and differences in activation pattern across age groups and experimental conditions. PLS determines time-varying distributed patterns of brain activity as a function of experimental variables, behavioral measures, and/or voxel activity from region of interests (ROIs). An identified pattern reflects activation changes across all regions of the brain simultaneously rather than tessellations of regions, thus ruling out the need for multiple comparison corrections. Moreover, PLS does not make any assumptions about how conditions collate to form a pattern, but rather pulls out contrasts that account for the most variance in the data. A detailed description of spatiotemporal PLS analysis for fMRI data has been given in previous reports (Salami et al., 2010, 2012). In brief, onset of each block of images (interference and control) was convolved with the SPM HRF function and averaged across blocks for each condition within each age group. A cross-block covariance matrix between changes in brain activity and experimental conditions (young-interference, young-control, old-interference, old-control) was then subjected to a mean-centering procedure, following Singular Value Decomposition (SVD), to identify a set of orthogonal latent variables (LVs), which represent linear combinations of the original variables. Each LV delineates cohesive patterns of brain activity related to experimental conditions and consists of Eigenvalues and two sets of saliences. Eigenvalues indicate the amount of cross-block covariance accounted for by each LV. The first set of saliencies (design saliences) represents a contrast across task conditions, and the second set of saliences (voxel saliencies) expresses how each voxel's pattern of signal changes reflects the task contrast. In addition, brain scores and design scores were calculated for each subject and LV across conditions. The former score reflects how much each subject contributes to the pattern expressed in each LV, and is obtained as a result of the dot product of each subject's image volume and the voxel saliencies of each LV. The latter score indicates how much each condition is related to the weighted voxels of each LV, and is calculated as the dot product of a subject's image volume and the design saliencies of each LV. For the seed PLS analysis, this procedure remained the same, except that the initial cross-correlation matrix was computed as the correlation between the activity of the seed region and activity in all other brain voxels across participants within each condition (see Krishnan et al., 2011). Accordingly, the first set of saliencies (seed saliencies) represents the pattern of covariance of the seed voxel and the rest of the brain across experimental conditions within each group. The variation across seed saliences indicates whether a given LV represents a similarity or difference in the brain-seed correlation across tasks/groups.

The statistical significance of each LV was assessed using permutation tests which involved reordering the rows of the data matrix and recalculating the LVs of the reordered matrix utilizing the same SVD approach. The number of times a singular value exceeds the original singular value yields the probability of significance of original LVs (McIntosh et al., 1996). In the present study, 500 permutations were performed. In addition, stability of voxel saliencies contributing to each LV was determined using bootstrap estimation of standard errors (SEs), using 100 bootstrap samples (Efron and Tibshirani, 1986). The Bootstrap

Ratio (BR), the ratio between voxel saliences and the estimated SEs, was computed and voxels with BR > 4 (approximately a Z-score of 4, corresponding to $p < 0.0001$; Efron and Tibshirani, 1986, two-tailed) were considered as reliable. All reliable clusters comprised at least 10 contiguous voxels, located at least 10 mm apart from each other. In addition, the upper and lower percentiles of the bootstrap distribution were used to generate 95% confidence intervals (CIs) around the brain and correlation scores to facilitate interpretation. For example, a significant difference between brain/correlation scores in different conditions is indicated by non-overlapping CIs. Similarly, brain/correlation scores were deemed unreliable when CIs overlapped with zero.

Two types of PLS analyses were carried out. First, task PLS was the primary analysis to investigate group differences in brain networks associated with the experimental variables in the MSIT. From this analysis as well as on the basis of past MSIT research (Bush et al., 2003), we identified seed ROIs to be used in a subsequent combined behavioral and functional connectivity analysis to examine whether (a) the functional relevance of regions reflecting reliable group differences depends on their connectivity to other brain regions; and (b) those connectivity patterns vary between age groups and are modulated by performance. Thus, task PLS assesses how brain activities are modulated across different conditions/groups, whereas seed PLS assesses how functional couplings between different brain regions are modulated across different conditions/groups as well as their relations to performance.

To further investigate age-related differences in brain function and structure, as well as their associations, a voxel-wise general linear model was set up for each participant and imaging modality, separately. For the fMRI data, each condition (interference and control) was modeled as a box-car function convolved with the hemodynamic response function. Subject-specific contrasts were taken into a second level random-effect model using two-sample t-tests to compare interference networks between the young and older groups. For the sMRI data, two-sample t-tests were carried out with smoothed modulated normalized GM volumes as the dependent variable between the age groups. To adjust for inter-gender variation in brain volume, a subject-specific total intracranial volume was computed by summing the GM, WM, and CSF segments, which was used as a covariate of no interest. For both analyses, local maxima with $p < 0.05$ (FWE corrected), with an extended threshold of 20 contiguous voxels ($K > 20$) were considered to be significant.

In a final set of analysis, functional and structural data from two age groups were investigated using an extension of independent component analysis (ICA) for multimodal neuroimaging data termed 'joint ICA' (jICA; Calhoun et al., 2006). This multivariate technique decomposes multiple subject-specific features (e.g. SPM contrast, GM volume) from different imaging modalities into a joint set of maximally spatially independent components. Additionally, jICA produces a set of coefficients, termed mixing coefficients, which represents how strong each subject contributes to the relationship expressed in each joint component. These mixing coefficients provide a straightforward mean to identify whether a depicted relationship in a component differs between age groups using two sample t-tests. However, such a measure does not simply capture age-related differences in either data type. Therefore, interpretation of results is facilitated by coefficient testing and by examining simple age-related differences in the original dataset. Here, a statistical parametric mapping contrast image reflecting interference vs. control and a smooth-normalized GM image for each subject (across the two age groups) served as input for jICA. As such, 18 independent components were estimated from the fused data (using minimum description length criteria; Calhoun et al., 2001); however, only one component depicted a significant difference (for loading parameters) between the two age groups ($p < 0.001$) and also reflected age-related changes for both functional and structural features. Regional effects contributing to each feature of the significant component were converted to Z-scores and considered reliable at $Z > 3$.

Results

Behavioral findings

2 (Age) × 2 (Condition) ANOVAs were conducted on the data for accuracy and latency for correct trials. Where appropriate, t-tests with Bonferroni correction were carried out. For accuracy (Fig. 1C), there was a main effect of condition ($F(3, 98) = 24.98$, $p < 0.0001$), a marginally significant effect of age ($F(3, 98) = 3.36$, $p = 0.068$), and a significant age × condition interaction ($F(3, 98) = 4.40$, $p < 0.05$). Accuracy was lower during interference than during control in older adults ($p < 0.0001$), but only marginally significant in the young ($p = 0.09$). Moreover, older adults were less accurate than the young during interference ($p < 0.05$), but not during control ($p = 0.95$). For RTs (Fig. 1B), there were significant main effects of condition ($F(3, 98) = 220.84$, $p < 0.0001$) and age ($F(3, 98) = 54.95$, $p < 0.0001$), but no significant interaction ($F < 1$). RTs were longer in the interference than in the control condition in both age groups ($p < 0.0001$), and longer in the older group than the younger group for both conditions ($p < 0.0001$).

fMRI findings

Task PLS

Two significant LVs were identified in the task PLS analysis. LV1 ($p < 0.0001$, Fig. 2A) accounted for 80% of the cross-block covariance and identified brain regions differentiating the interference from the control condition. This pattern was similarly expressed in younger and older adults (Fig. 2B). Regions showing greater activity during interference (Fig. 2A, red color) were dominated by a fronto-parietal network, including superior and middle frontal gyrus, superior and inferior parietal lobule, occipital gyrus, pre-SMA, fusiform gyrus, anterior and middle cingulate cortex, putamen, and caudate, bilaterally. Brain regions showing relatively more activity during the control condition (Fig. 2A, blue color) included bilateral medial frontal gyrus, bilateral middle temporal gyrus, bilateral angular gyrus, bilateral precuneus, left cuneus, bilateral parahippocampus, left orbitofrontal cortex, and posterior cingulate gyrus (Table 1).

LV2 ($p < 0.005$, Fig. 2E) accounted for 19.6% of the cross-block covariance and also separated the interference and control conditions across age groups (Fig. 2F). For one set of regions, activity was increased during interference compared to control for the older group. For the younger group, the change in activity between the two conditions was in the opposite direction. In addition, the within-condition scores differed between age groups during both control and interference. Those regions (Fig. 2E, red color) exhibiting greater activity during interference for the older group included DLPFC, dACC, left inferior parietal cortex, left calcarine, right lingual gyrus, right precuneus, SMA, and bilateral middle temporal gyrus. The signal changes for selected regional maxima in dACC and DLPFC are shown in Figs. 2G, H (reliable signal differences during interference but not during control). In contrast, no region showed increased activity during interference compared to control for the young group. Consistent with the LV2, a univariate second-order random effect analysis revealed greater activation in the older compared to the younger group during interference in the same regions (including DLPFC and dACC), as revealed by the PLS analysis (Table 2). This supplementary analysis further substantiates that the majority of regions identified by LV2 exhibited greater interference-related activity in older adults.

Seed PLS

The choice of seed regions for the functional connectivity analysis was based on two criteria: (a) Located in PFC or ACC based on previous evidence of a key role of these regions for interference resolution in the MSIT (Bush and Shin, 2006; Bush et al., 2003); and (b) Reliable modulation of activity across tasks for one or both age groups. The task PLS

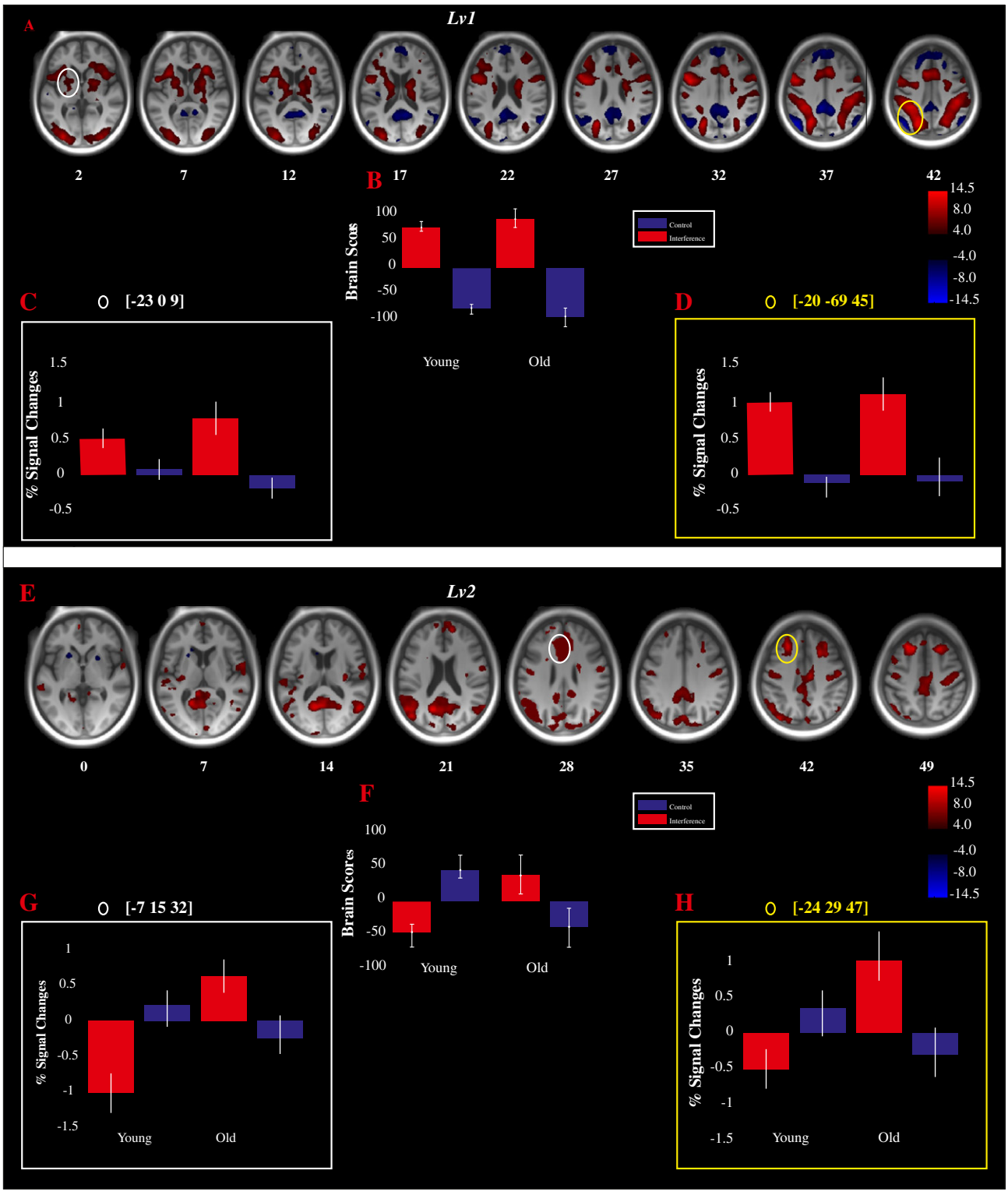

Fig. 2. Singular images and brain scores for the two significant latent variables (LVs). (A, E) Singular images for LV1 and LV2, which reflect reliable regions (Bootstrap Ratio [BSR] > 4; range is indicated by the color bar) contributing to the pattern identified in each LV. For LV1, red color is associated with regions exhibiting greater activity during interference than during control across both age groups, whereas blue color indicates brain regions reflecting greater activity during control than during interference across both age groups. For LV2, red color is associated with regions reflecting greater activity during interference in the old group than in the young, whereas blue color indicates brain regions exhibiting greater activity during interference in the young group than in the old. (B, F) Brain scores for LV1 and LV2, reflecting common and age-specific interference and control networks. Error bars denote 95% confidence intervals. Circles indicate left DLPFC and left dorsal ACC, linked to greater interference effects in older compared to younger adults. (C, D) Signal changes in two selective regions reliably contributing to LV1 (i.e. greater interference compared to control in both age groups). (G, H) Signal changes in two seed regions strongly contributing to LV2 (i.e. greater interference in old compared to young).

analyses revealed that the elderly group over-recruited left DLPFC as well as left dACC during the interference, but not the control, condition (see Figs. 2G and H); these regions strongly contributed to the pattern for LV2 (Table 2). Using seed PLS, we investigated within a single analysis: (a) How the seed regions were functionally connected with other brain regions and whether these patterns of connectivity were

Table 1
Regions from LV1 showing interference vs. control network equally expressed for both age groups.

Regions	X Y Z	BSR
Positive direction		
L-sup-frontal	[−26 −6 63]	14.50
L-sup-parietal	[−20 −69 45]	13.80
R-sup-frontal	[27 −5 59]	13.02
L-inf-parietal	[−36 −42 45]	12.81
R-sup-parietal	[27 −62 53]	12.50
L-fusiform	[−39 −75 −17]	12.30
L-inf-occipital	[−36 −84 −6]	12.25
R-inf-parietal	[32 −53 50]	12.10
L-supp-motor	[0 11 50]	11.91
R-fusiform	[39 −54 −18]	11.61
L-mid-occipital	[−27 −69 30]	11.58
R-inf-occipital	[32 −86 −9]	11.22
R-supp-motor	[8 −2 66]	10.32
L-mid-cingulum	[−8 15 42]	10.01
R-mid-cingulum	[6 18 39]	9.93
R-caudate	[17 −6 18]	8.35
L-putamen	[−23 0 9]	7.71
R-putamen	[26 −2 6]	7.57
R-mid-frontal	[36 50 27]	7.55
L-inf-frontal	[−45 33 26]	7.31
L-mid-frontal	[−41 39 33]	6.74
L-insula	[−41 17 −2]	6.72
L-ant-cingulate	[−8 24 29]	5.78
L-mid_frontal	[−33 50 18]	5.35
R-inf-frontal	[48 38 26]	4.25
R-mid-frontal	[48 3 53]	4.21
Negative direction		
L-angular	[−45 −75 39]	11.78
L-mid/post-cingulum	[−6 −42 38]	8.88
R-angular	[50 −69 42]	8.60
L-medial-frontal	[−5 45 50]	8.15
L-mid-temporal	[−56 −8 −14]	7.93
L-parahippocampus	[−27 −33 −12]	7.40
R-mid-temporal	[53 −6 −15]	7.06
R-parahippocampus	[30 −33 −14]	6.72
L_cuneus	[−3 −96 20]	5.92
R-medial-frontal	[6 57 36]	5.70
R-hippocampus	[23 −9 −18]	5.48
R-cuneus	[14 −89 41]	5.32
L-hippocampus	[−21 −11 −14]	4.98

BSR: Bootstrap Ratio.
BSR > 4, $p < 0.0001$.

modulated by task performance; and (b) Whether these functional connectivity networks as well as their relations with performance differed across age groups.

Table 2
Regions from LV2 reflecting group-specific interference networks and corresponding regions from SPM reflecting the interference network.

Regions	X Y Z	BSR	SPM (X Y Z)	SPM T
Positive direction				
L-calcarine	[−15 −65 20]	7.29	[−15 −64 19]	6.23
L-mid-frontal	[−24 29 47]	7.11	[−24 28 46]	6.07
L-sup-frontal	[−18 20 60]	5.46	[−28 19 60]	5.22
L-fusiform	[−26 −45 −9]	7.00	[−25 −45 −9]	5.98
L-ant-cingulate	[−7 15 32]	6.85	[−3 12 30]	5.47
L-mid-occipital	[−38 −78 42]	6.29	[−27 −78 42]	4.73
R-lingual	[11 −80 −12]	6.36	[10 −79 −12]	5.13
R-sup-frontal	[21 26 47]	6.17	[21 25 46]	4.82
R-mid-temporal	[54 −62 14]	5.99	[54 −61 13]	4.94
R-mid-cingulum	[9 −15 44]	5.35	[9 −15 43]	4.97
R-paracentral	[9 −38 69]	5.10	[9 −37 69]	5.09
R-precuneus	[6 −50 62]	5.09	[6 −49 61]	4.74
Left-sup-parietal	[−24 −80 47]	5.03	[−24 −79 46]	5.82
Left-paracentral	[−2 −21 62]	5.02	[−2 −21 61]	5.35
Left-sup-motor	[−6 23 65]	5.01	[−6 22 64]	4.12

BSR: Bootstrap Ratio.
BSR > 4, $p < 0.0001$.

Left DLPFC (BA 9/8)

Using left DLPFC as seed (X Y Z = −24 29 47), the functional connectivity analysis yielded two significant LVs. LV1 ($p < 0.001$) demonstrated positive seed and performance correlations for accuracy in the interference condition among the young. In contrast, a non-reliable positive seed correlation and a negative performance correlation for accuracy were observed during interference in the older adults (Fig. 3B). No reliable correlation was observed for RT in either group. Moreover, no reliable correlation was observed for RT and accuracy during the control condition. Note that, although both younger and older adults engaged the network (LV1; Fig. 3B; overlapping CIs across yellow bars), the correlation with seed was reliable in the young, but not for the older adults (i.e. yellow bar's CI in the older adults crosses zero). Critically, the correlation with accuracy was remarkably different across two groups (Fig. 3B; non-overlapping CIs across blue bars). The network (Fig. 3A; regions in red color) demonstrating positive seed and performance correlations for accuracy in the young engaged primarily anterior parts of the brain, including right middle frontal gyrus, ACC, bilateral inferior frontal gyrus as well as caudate, pallidum, and right thalamus. In addition, this network included a few posterior brain regions, encompassing left fusiform and left superior and middle occipital gyrus (Table 3). LV2 ($p < 0.05$) demonstrated positive seed and behavioral correlations for accuracy and a negative correlation for RT in the interference condition for the older group only. Both younger and older adults engaged the network (LV2; Fig. 3D; overlapping CIs across yellow bars), but the correlation with seed for the young was weak and non-reliable (i.e. yellow bar's CI in the young crosses zero). Critically, correlations with both accuracy and RT were remarkably different between two groups (Fig. 3D; non-overlapping CIs across blue bars and across green bars). This network (Fig. 3C; regions in red color) involved more posterior parts of the brain, including right lingual gyrus and left parietal gyrus extendeding into left angular gyrus. Moreover, this network included left pre/post central gyrus, left SMA, left middle temporal gyrus, left superior frontal gyrus and medial frontal gyrus bilaterally (Table 3). Again, no reliable correlations were observed for RT and accuracy during the control condition.

Left dACC (BA 32/24)

The functional connectivity analysis with left dACC as seed (X Y Z = −7 15 32) also revealed two significant LVs. LV1 ($p < 0.001$) exhibited positive seed and performance correlations for accuracy during interference in the young group only. Both young and old engaged the network (LV1; Fig. 4B; overlapping CIs across yellow bars), but the correlation with seed in the older adults was weak and non-reliable. Again, the correlation with accuracy was remarkably different across two groups (Fig. 4B; non-overlapping CIs across blue bars). This network (Fig. 4A; regions in red color) also involved more anterior parts of the brain, including bilateral middle, superior, and inferior frontal gyrus. Moreover, this network including right superior parietal cortex, left precuneus, left pallidum, and right thalamus (Table 4). LV2 ($p < 0.01$) demonstrated positive seed and behavioral correlations for accuracy and a negative performance correlation for RT during interference in the older adults. This network did not reliably correlate with seed or behavioral measures in the young, and correlations with both accuracy and RT were significantly different across age groups (Fig. 4D; non-overlapping CIs across blue bars and across green bars). Regions demonstrating reliable correlations (Fig. 4C; regions in red color) with seed and positive-/-negative correlations with accuracy/RT included bilateral superior frontal cortex, bilateral middle cingulum, left angular gyrus, bilateral lingual gyrus, left middle temporal gyrus, left pre/post central gyrus, left SMA, and left medial frontal gyrus (Table 4). Neither network exhibited a reliable correlation with accuracy or RT during the control condition.

Given the strikingly similar networks anchored by DLPFC and dACC, we refer to both regions as seeds in the remaining text.

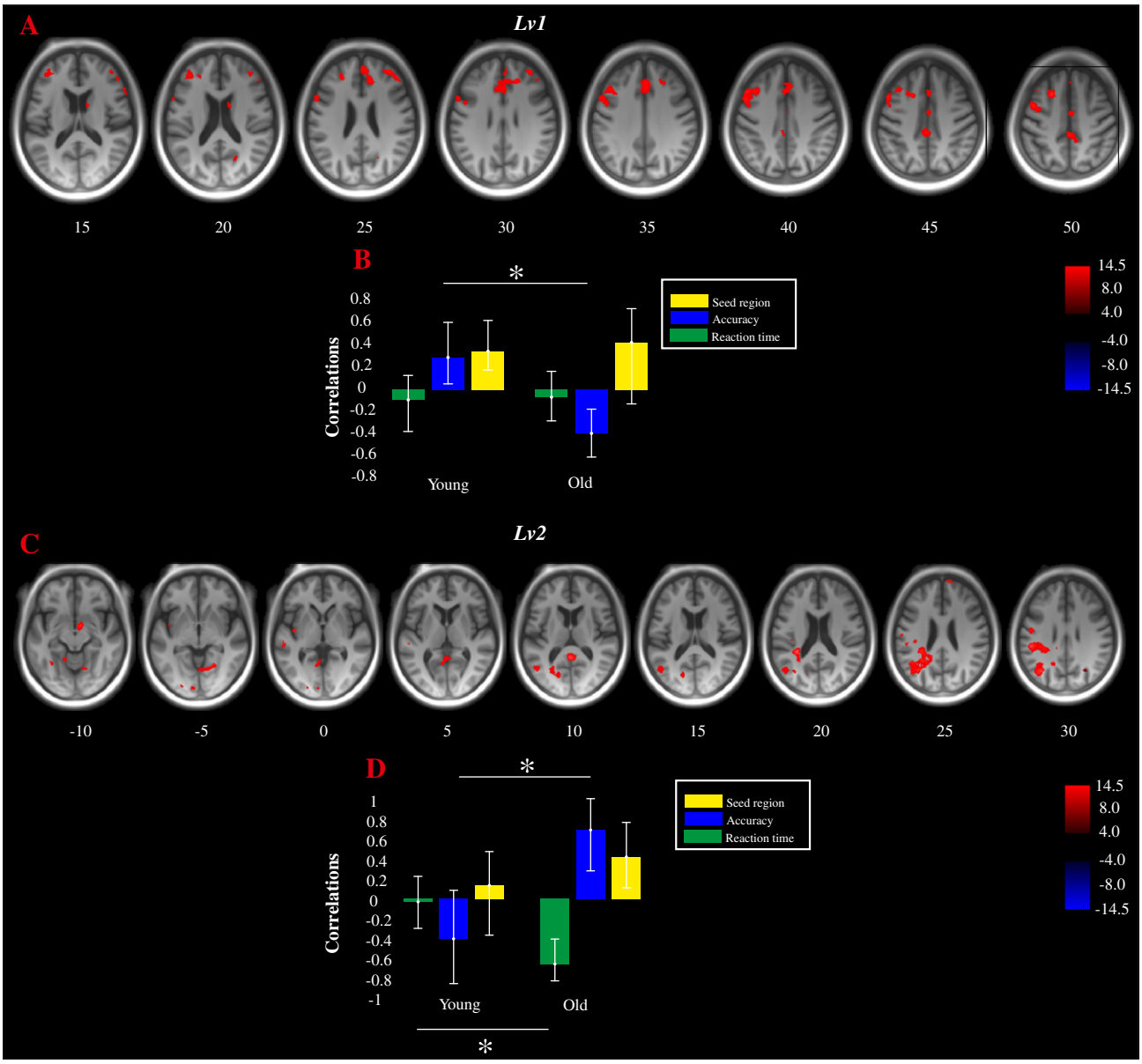

Fig. 3. Singular images, behavioral and seed LVs for DLPFC (−24 29 47) extracted from LV2 in the task PLS analysis. (A, C) Singular images for LV1 and LV2, which exhibited reliable correlations with the seed and behavioral measures (accuracy and RT) during interference. Regions with BSR > 4 (corresponding approximately to $p < 10^{-4}$) are shown in red color. (B, D) Seed and behavioral LVs during interference. Error bars denote 95% confidence intervals defined by standard errors of the bootstrap estimates. Error bars crossing zero indicate non-reliable contributions of seed or behavioral measures. For LV1 (B), regions shown in red color (A) reflect positive correlations with the seed (DLPFC, yellow bar) and accuracy (blue bar) during interference in the young and a negative correlation with accuracy (blue bar) during interference in the old. For LV2 (D), regions depicted in red color (C) reflect a positive correlation with the seed (DLPFC, yellow bar), a positive correlation with accuracy (blue bar) during interference, and a negative correlation with RT (green bar) during interference in the old only. Asterisks indicate reliable age differences for accuracy and reaction time.

The observation of two distinct functional networks differentially modulated by performance across young and older adults along with less efficient interference resolution (i.e. lower accuracy and longer reaction time) in older adults suggests that the network that promoted interference resolution in the old was not as efficient as that recruited by the young. Although these patterns may reflect general age differences, there might be individual differences within the older sample. Specifically, elderly persons with better interference resolution (i.e. old-high) may engage the same network as their younger counterparts. We tested this possibility by identifying a high-performing older subgroup based on a median-split analysis (n = 12). We then examined whether this group showed a similar pattern of functional connectivity that promoted interference resolution in young. Indeed, this analysis confirmed that the old-high group engaged the same functional network as the young (Fig. 5). By contrast, the remaining old adults with lower accuracy during interference resolution (i.e. old-low) did not recruit this network reliably (Fig. 5). Furthermore, this network was positively and negatively correlated with accuracy during interference in the old-high and old-low groups, respectively.

Structural MRI analysis

Structural analysis of GM volumes revealed marked age-related reductions in several regions, including inferior, middle, and superior frontal cortex, left ACC, middle cingulum, left superior/inferior parietal cortex, left cuneus, and right thalamus (Table 5). Importantly, these regions overlap greatly with the functional networks connected with the seeds in the younger group (spatial correlation with LV1 (DLPFC):

Table 3
Regions of functional connectivity reflecting positive correlation with seed (DLPFC; −24 29 47) in young (LV1) and old (LV2).

Regions	X Y Z	BSR
LV1		
L-sup-occipital	[−15 −83 42]	10.73
L-inf-frontal	[−45 17 −6]	9.57
L-middle-occipital	[−33 −86 21]	8.90
R-mid-frontal	[36 47 29]	7.77
L-supramarginal	[−62 −20 21]	7.63
L-mid-frontal	[−39 21 38]	7.40
L-fusiform	[−26 −62 −14]	7.29
R-ant-cingulum	[12 35 27]	6.95
L-sup-frontal	[−14 30 −24]	6.95
R-inf-frontal	[45 39 27]	6.95
R-caudate	[12 3 18]	6.87
L-inf-frontal	[−57 12 24]	6.82
L-mid-frontal	[−38 41 20]	6.65
R-sup-frontal	[11 41 54]	6.65
R-ant-cingulum	[5 50 26]	6.48
L-ant-cingulum	[−9 24 32]	6.05
L-inf-frontal	[−50 30 −6]	5.97
L-inf-frontal	[−39 44 6]	5.83
L-pallidum	[−11 6 3]	5.79
R-inf-frontal	[60 24 15]	5.75
R-ant-cingulum	[2 45 12]	5.67
L-mid-frontal	[−35 26 48]	5.39
L-ant-cingulum	[−3 29 15]	5.11
LV2		
L-angular	[−45 −75 39]	5.85
L-mid-occipital	[−36 −66 29]	5.80
L-sup-parietal	[−33 −65 57]	5.79
R-mid-occipital	[36 −75 41]	5.76
L-sup-frontal	[−15 26 44]	5.73
L-precuneus	[2 −48 9]	5.72
L-precuneus	[−14 −68 60]	5.71
L-sup-frontal	[−18 20 62]	5.70
L-supramarginal	[−51 −32 30]	5.50
L-supp-motor	[−2 −8 74]	4.70
R-lingual	[14 −63 −8]	4.70
L-mid-temporal	[−56 −27 2]	4.47
L-calcarine	[−18 −72 14]	4.35
L-angular	[−44 −56 27]	4.34
L-mid-cingulum	[−12 −36 36]	4.23
R-medial-frontal	[8 54 42]	4.01

BSR: Bootstrap Ratio.
BSR > 4, $p < 0.0001$.

$r = 0.68$; $p < 0.0001$; spatial correlation with LV1 (dACC): $r = 0.72$; $p < 0.001$), but not with the functional networks connected with the seeds in the older group (spatial correlation with LV2 (DLPFC & dACC): $r = 0.07$; $p > 0.1$). Additional analysis using a mask of the network functionally connected with the seed in the elderly (LV2) revealed that GM volumes in almost all of these regions were highly preserved even using a more liberal threshold ($p < 0.001$; uncorrected). The only region within the network, that exhibited age-related GM loss was left middle cingulum (X Y Z = −5 15 41; $p < 0.001$).

Structure–function integration

Consequently, we examined whether age-related differences in functional activation patterns could be distally accounted for by structural differences. The jICA identified one joint component depicting a relationship between GM volume and functional activation that was significantly different between the younger and older age groups (Fig. 6; Young: mean mixing coefficient = 0.0029 ± 0.01; Old: mean mixing coefficient = 0.0217 ± 0.021; $t_{49} = 4.08$, $p < 0.0001$). The observation of age-related differences in mixing coefficients suggests that the relationships in the data types (i.e. relation between interference network and GM volume) expressed in the component differ across age and required further investigation. However, it is also important to visualize which brain regions in each feature that showed the largest age-related differences in order to facilitate interpretation. The spatial extent of the fMRI feature (reflecting the interference network) revealed increased functional activity in several areas, dominated by posterior parts of the brain (Fig. 6, Table 6). Interestingly, these regions overlap strongly with the network linked to seed regions more so in the older group (LV2 from the seed analyses, spatial correlation with LV2 (DLPFC): $r = 0.55$; $p < 0.0001$; spatial correlation with LV2 (dACC): $r = 0.57$; $p < 0.001$). Accordingly, the GM feature of the significant component depicted GM volume loss in several brain regions reflecting age-related GM volume differences in the structural analysis (Fig. 6, Table 6; spatial correlation with GM atrophy: $r = 0.71$; $p < 0.0001$). Taken together, our ICA result identified an age-sensitive component in which GM volume differences were associated with increases in functional connectivity within the fronto-parietal circuitry.

Discussion

We explored age differences in the neural correlates of interference resolution, an operation by which the brain attempts to limit processing to task-relevant information while ignoring irrelevant information. We characterized the behavioral implications of neural activity patterns during the MSIT in young and older adults, and provide novel evidence of functional reorganization of neural networks to support interference resolution in aging.

Older adults were slower during both interference and control conditions. Further, older adults were less accurate during interference, but not during control, compared to their younger counterparts. This finding suggests that the size of the interference effect was larger in older subjects than in younger subjects. This finding is in contrast with some studies, which failed to find a significant interaction between age and stimulus congruence (Huang et al., 2012; Langenecker et al., 2004; Schulte et al., 2009; Zysset et al., 2007). One possible interpretation of the increased proneness to interference in aging found in the current study, may be related to the nature of the MSIT task, which taxes multiple sources of interferences. Whereas our behavioral findings are consistent with the notion of increased proneness to interference in aging (Prakash et al., 2009; See and Ryan, 1995; West, 1996), they conflict with the suggestion that susceptibility to interference in older age is merely driven by general slowing (Uttl and Graf, 1997; Verhaeghen and De Meersman, 1998). Thus, the observation of reduced performance in older adults during the interference condition, but not during the control condition, suggests that stimulus–response conflict is affected in aging.

LV1 from the primary task PLS analysis yielded similarities in activation patterns during interference across age groups. The fact that the age-common network (LV1) accounted for a considerably larger portion of the cross-block covariance than the age-specific network (LV2) indicates that age similarities in activation patterns were predominant. Consistent with increased RT during interference across age, the pattern in LV1 suggests that activity increased in both age groups when the number's position was a source of conflicting identity information. This interference network involved large portions of fronto-parietal cortex, pre-SMA, ACC, and basal ganglia, areas that have been implicated in interference resolution (Adleman et al., 2002; Banich et al., 2000; Bush and Shin, 2006; Carter et al., 1995; Huang et al., 2012; Taylor et al., 1997). Inferior and middle frontal gyrus has been associated with top–down attention (Hopfinger et al., 2000), attention to targets (Corbetta and Shulman, 2002), and response inhibition and selection (Aron et al., 2004), and ACC has been implicated in several control processes, including error detection, response selection, and inhibition (Bush et al., 2000, 2002; Williams et al., 2004). Finally, pre-SMA has been identified as a region critical to response inhibition (Garavan et al., 1999; Humberstone et al., 1997). By contrast, the network engaged during the control condition included regions highly resembling the default mode network (DMN), which reflects intrinsic properties of the brain's functional organization (Gusnard et al., 2001; Raichle et al., 2001).

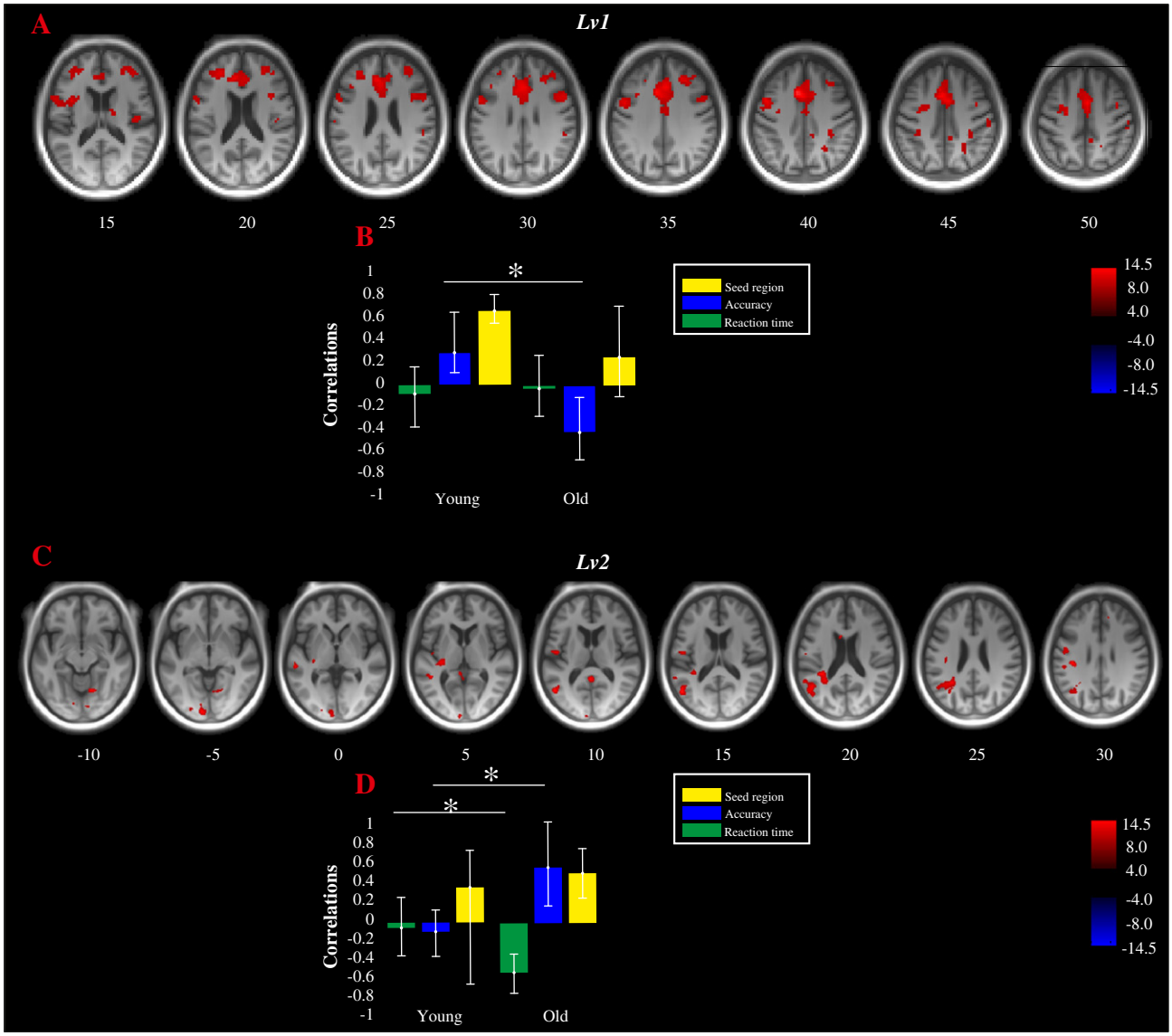

Fig. 4. Singular images, behavioral and seed LVs for dACC (−7 15 32) extracted from LV2 in task PLS analysis (for details, see Fig. 3).

Activation of the DMN during tasks with minimal cognitive demands has been reported previously (Van Dijk et al., 2010; Zysset et al., 2007).

Despite largely overlapping activation patterns across age groups, age differences in brain activation during interference were also observed. Consistent with a larger interference effect in the older group, LV2 revealed a network with increased activation during interference for the old only. This network involved DLPFC, ACC, precuneus, left inferior parietal cortex, left calcarine, pre-SMA, and bilateral temporal gyrus. Note that most of the regions showing greater activity in the old are located in close proximity to regions yielding similar activity in both age groups. The observation of age-related over-recruitment during interference is consistent with past research (Gazzaley et al., 2005, 2008; Huang et al., 2012; Zysset et al., 2007). Age-related increases of PFC activity have been associated with successful inhibition (Nielson et al., 2002), and age-related increases in ACC activity have been attributed to heightened potential for error in old age (Milham et al., 2002), consistent with our observation of less proficient interference resolution in the older adults. Although PFC and ACC exhibited age-related functional increases during interference, they did not show any reliable age differences during the control condition. However, LV2 also reflected an interaction effect. Some of the regions that showed greater activity during interference than control in older adults exhibited the opposite pattern in the young. Interestingly, some of these regions (e.g. parietal cortex, temporal cortex, and precuneus) fall into the known topology of the DMN (Buckner et al., 2008; Raichle and Snyder, 2007). Thus, LV2 encompasses parts of the DMN that were suppressed in the young, but upregulated in the old during interference. This observation is consistent with previous reports demonstrating that older adults are less successful in suppressing DMN activity when performing cognitively demanding tasks (Persson et al., 2007; Prakash et al., 2012). Thus, our results suggest that, although most parts of the DMN were deactivated during interference resolution in both age groups (i.e. control condition in LV1), some parts were not properly deactivated during interference in older adults (LV2).

Further, we employed multivariate seed PLS to assess the functional connectivity and cognitive relevance of the networks anchored by DLPFC and dACC. Two distinct networks were differentially modulated by performance across age groups. For the young, the seed regions were functionally connected to more anterior parts of the brain, including inferior and middle frontal gyrus, ACC, right thalamus, caudate, and pallidum. The greater engagement of the network functionally connected to the seeds was associated with higher accuracy in the

Table 4
Regions of functional connectivity reflecting positive correlation with seed (LACC; −7 15 32) in young (LV1) and old (LV2).

Regions	X Y Z	BSR
LV1		
L-mid-cingulum	[−9 18 39]	19.28
L-ant-cingulum	[−9 35 21]	12.93
L-middle-frontal	[−27 41 21]	11.16
R-middle-frontal	[29 32 33]	11.16
L-inf-frontal	[−45 17 −4]	10.77
L-sup-frontal	[−23 −9 53]	10.33
R-inf-frontal	[51 12 29]	9.58
R-ant-cingulum	[6 36 23]	9.54
L-inf-frontal	[−57 9 14]	9.28
R-mid-frontal	[39 39 30]	8.73
L-inf-frontal	[−33 32 5]	8.62
R-inf-frontal	[53 39 8]	8.43
L-sup-frontal	[−14 30 −24]	8.12
L-mid-frontal	[−38 42 17]	7.98
L-supramarginal	[−60 −20 24]	7.71
R-caudate	[9 5 14]	6.78
L-fusiform	[−38 −35 −20]	6.36
L-sup-occipital	[−23 −83 39]	6.27
L-fusiform	[−45 −57 −15]	5.59
L-sup-occipital	[−11 −78 44]	5.35
L-pallidum	[−24 −9 3]	5.27
L-pallidum	[−17 6 −2]	5.10
L-inf-frontal	[−50 33 −6]	5.07
LV2		
L-sup-frontal	[−12 27 42]	6.76
R-sup-frontal	[14 42 33]	6.32
R-lingual	[15 −63 −8]	5.91
L-mid-temporal	[−51 −27 2]	5.76
L-calcarine	[−9 −95 −6]	5.42
R-medial-frontal	[11 35 41]	5.11
L-mid-temporal	[−57 −30 0]	4.87
L-supp-motor	[−6 −8 68]	4.73
L-angular	[−38 −56 26]	4.48
L-sup-parietal	[−30 −65 55]	4.47
L-precuneus	[−12 −44 42]	4.41
R-mid-occipital	[36 −75 40]	4.37
L-mid-occipital	[−36 −66 29]	4.12
L-supramarginal	[−51 −30 30]	4.07
L-precuneus	[−12 −68 61]	4.05

BSR: Bootstrap Ratio.
BSR > 4, p < 0.0001.

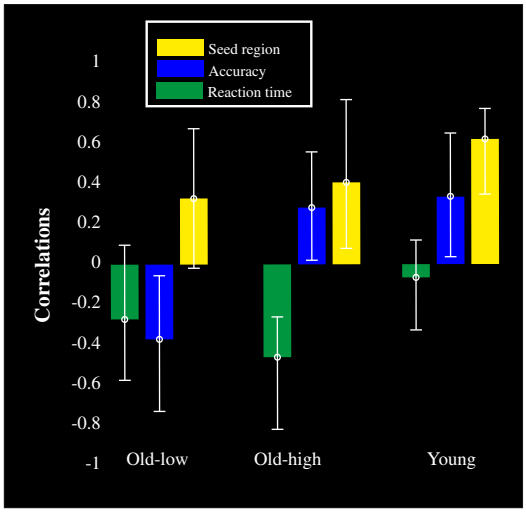

Fig. 5. Seed and behavioral LVs for dACC (−7 15 32) during interference as a function of behavioral proficiency. Older adults were subdivided into two groups of high- and low-performers (old-high vs. old-low) according to a median-split analysis based on accuracy during interference resolution. Both young and old-high groups exhibited positive seed and performance correlations for accuracy during interference, whereas the correlation with seed in the old-low group was non-reliable. The correlation with accuracy was remarkably different between the old-high/young group and the old-low group.

Table 5
Regions showing age-related GM loss.

Regions	X Y Z	T value	Cluster size
L-inf-frontal	[−45 17 −6]	8.05	684
L-ant-cingulum	[0 51 2]	8.38	5941
L-ant-cingulum	[−2 39 27]	7.35	Subreg
L-mid-cingulum	[−2 5 47]	6.93	Subreg
L-sup-temporal	[−47 0 −2]	8.30	684
L-mid-frontal	[−26 35 45]	8.02	383
L-mid-frontal	[−26 26 52]	6.71	Subreg
L-mid-frontal	[−41 24 32]	5.42	Subreg
L-mid-temporal	[−26 35 45]	7.87	383
R-mid-temporal	[56 −63 15]	7.18	707
L-inf-parietal	[−45 −42 53]	7.02	158
L-sup-frontal	[−14 30 −24]	6.66	60
L-sup-frontal	[−14 47 −21]	6.49	50
R-thalamus	[2 −12 6]	6.33	78
L-postcentral	[−41 −17 53]	6.27	86
L-mid-temporal	[−57 −60 18]	5.92	108
L-sup-frontal	[−14 48 43]	5.85	20
R-caudate	[14 9 9]	5.48	30
L-inf-frontal	[−50 33 −8]	5.42	65
R-inf-frontal	[42 32 16]	5.27	30
L-pallidum	[−17 6 −3]	5.26	27

p < 0.05 (FWE corrected), K > 20.

interference condition for the young. Older adults, however, did not recruit this network reliably, and their accuracy was negatively correlated with the network. By contrast, a second network, which was also functionally connected to the seeds, was expressed in older adults only. This network involved posterior parts of the brain, including bilateral parietal cortex, left middle temporal gyrus, right lingual gyrus, as well as left superior frontal gyrus and pre-SMA. Interestingly, greater engagement of this network was associated with higher accuracy and faster RT during interference in older adults. Note that for both networks, the correlation with accuracy was significantly different for the two age groups. The observation of two distinct functional networks differentially modulated by performance in younger and older adults provides evidence in support of functional reorganization in aging (Bennett et al., 2001; Reuter-Lorenz and Lustig, 2005; Tisserand et al., 2005). One possibility is that use of this circuitry compensated for the weakened state of the primary neural network utilized by the young (Stern, 2002, 2009). However, although it facilitated performance, recruitment of the alternate network was still associated with less efficient performance in the older adults (Zarahn et al., 2007). A unique pattern of neural activity that facilitates performance in an age-specific manner supports the view of brain compensation in aging (Grady, 2008, for review see Grady, 2012). However, note that older persons who performed at a high level during interference engaged the same network as the young, whereas those older persons who had lower accuracy levels did not. Thus, not only chronological age, but also performance level, needs to be considered in accounting for the current differences in connectivity. This pattern is consistent with previous observations from fMRI research on the load-dependent modulation of the BOLD signal during spatial (Nagel et al., 2009) and verbal (Nagel et al., 2011) working memory. Specifically a "youth-like" pattern of brain activation or connectivity seems to be associated with proficient performance in working memory and interference resolution alike.

Conflict resolution has been associated with increased activation of both an anterior executive control system and a posterior attention system. The former includes prefrontal regions and has been associated with conflict detection and resolution (Harrison et al., 2005; MacDonald et al., 2000). The latter involves parietal regions and has been linked to top–down attentional control, perceptual selection, and stimulus attribute identification (Casey et al., 2000; Milham et al., 2002). On this view, increased connectivity to the parietal network in older adults may reflect greater engagement of top–down attentional processes,

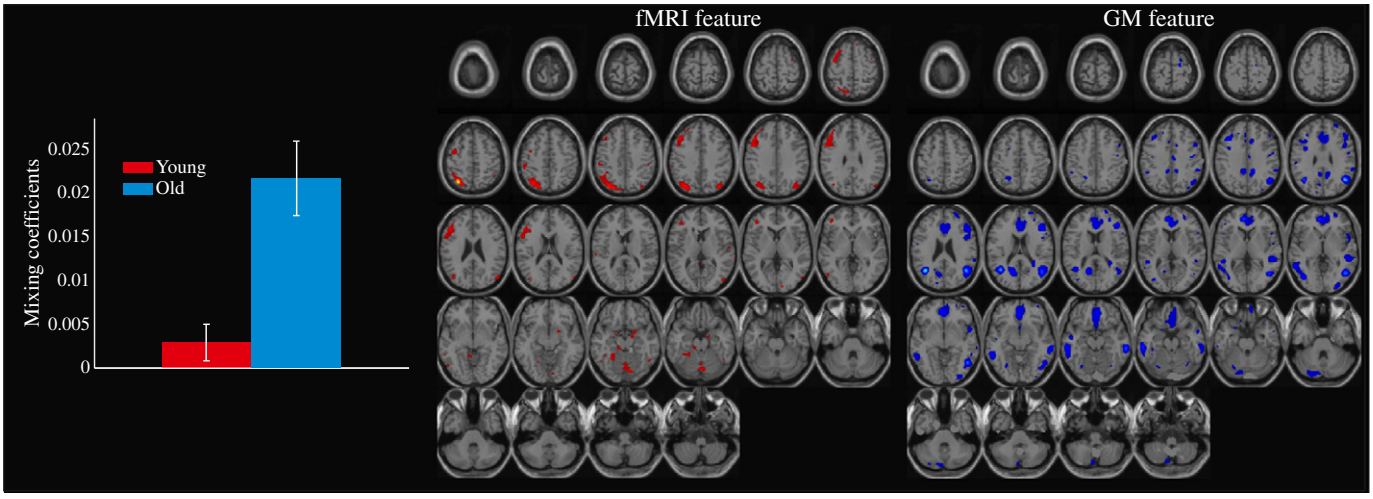

Fig. 6. Spatial structures (fMRI and GM features) of joint component observed across participants (Z = 2.5) and results of t-test for age group on jICA mixing coefficients. The left most column shows a graph comparing averaged mixing coefficients between age groups (mixing coefficients delineate how strong the association between two features is expressed in each group). The middle column reflects functionally-integrated regions associated with interference. The right most column shows the map of age-related GM volume differences.

and increased dependence of such processes to resolve interference. Previous studies have found age-related upregulation of parietal activation during a variety of cognitive tasks (Davis et al., 2008; Fera et al., 2005; Heuninckx et al., 2008), including interference tasks (Huang et al., 2012; Milham et al., 2002; Zysset et al., 2007). In particular, a recent study by Huang et al. (2012) reported age-related functional increases in left or right parietal cortex, depending on the nature of the conflict task. Interestingly, an elevated level of parietal activation was negatively correlated with latency, suggesting a possible compensatory mechanism. Consistently, we also observed age-related increases in functional connectivity to the parietal cortex, which promoted interference resolution in older adults. In the current study, greater engagement of this network was not only negatively correlated with RT, but also positively correlated with accuracy. In contrast, Huang and colleagues did not find age differences in accuracy, whereas older adults in our study were less accurate during interference supporting previously reported age-related deficits in inhibitory function (Hasher and Zacks, 1988; See and Ryan, 1995). Such differences in results could stem from the use of different paradigms (taxing task-specific interference vs. general interference) and methodology (regional activation level vs. network coupling level) adopted in the two studies. To the best of our knowledge, our study is the first to demonstrate age-related neural differences during interference resolution at the network level.

Table 6
MNI coordinates for fMRI and GM MRI features of the jICA component reflecting significant differences between age groups.

Regions	X Y Z	Z value	Cluster size
fMRI feature			
L-sup-parietal	[−33 −65 57]	11.09	1834
L-precuneus	[−14 −69 61]	4.06	Subreg
L-angular	[−45 −61 46]	3.70	Subreg
R-mid-occipital	[36 −75 41]	5.66	268
L-mid-frontal	[−48 24 39]	5.50	1416
L-mid-occipital	[−36 −66 29]	4.22	49
L-mid-occipital	[−42 −74 24]	3.58	Subreg
R-lingual	[14 −63 −8]	3.57	20
L-supp-motor	[0 −5 74]	3.05	11
sMRI feature			
L-mid-temporal	[−41 −60 24]	12.76	1116
L-mid-temporal	[−56 −58 18]	12.03	Subreg
R-mid-temporal	[40 −60 24]	11.33	2363
R-mid-temporal	[47 −62 −3]	9.71	3063
L-ant-cingulum	[−9 47 5]	8.80	1737
L-ant-cingulum	[0 36 12]	6.09	Subreg
L-ant-cingulum	[−2 27 22]	5.82	Subreg
L-mid-cingulum	[−8 17 39]	3.32	Subreg
R-inf-frontal	[42 33 17]	7.79	287
L-mid/inf-frontal	[−41 24 35]	6.17	621
L-mid-frontal	[−33 33 30]	4.06	Subreg
L-inf-parietal	[−51 −45 41]	4.99	87
L-mid/sup-temporal	[−53 −2 −10]	4.35	117
L-caudate	[−11 18 0]	3.69	12
L-sup-frontal	[−14 26 −23]	3.69	50
R-Caudate	[9 6 9]	3.00	10

Subreg: Subregion.
z > 3, K > 10.

Our observation of two distinct neural networks facilitating performance in young and older adults, respectively, may suggest age differences in strategy use when resolving conflict. Studies using transcranial magnetic simulation reveal that a specific cognitive process can be implemented in the brain in multiple ways (Lee et al., 2003; for review see Pascual-Leone et al., 2005). Toward this end, our results suggest that different brain implementations of conflict resolution are differentially vulnerable to aging. Younger adults efficiently resolve conflict by engaging a frontal executive network; this network may be vulnerable to aging due to frontal atrophy. The posterior attention network may be more resilient to aging than the frontal executive network (Kalpouzos et al., 2009), and thus, proficient interference resolution is accomplished using this network in older adults. As discussed below, the current analysis of structural brain data is in agreement with these propositions.

Consistent with other structural imaging studies in aging (Good et al., 2001; Nyberg et al., 2010; Raz et al., 2005), we found age-related volume differences in several regions, particularly in anterior parts of the brain. Interestingly, these regions overlapped greatly with the functional networks connected with the seeds in the young. Most earlier studies reporting age-related neural reorganization in various cognitive domains did not provide evidence regarding the role of the morphological substrate possibly underling functional reorganization. Still, some studies suggest that age-related differences in regional GM volume may locally account for age-related regional alterations in functional responses (e.g. Kalpouzos et al., 2011; Salami et al., 2012; Voss et al., 2008). However, an examination of the full set of brain regions connecting the two imaging modalities (e.g. distal effect) and reflecting joint information has been lacking. In the current study, jICA revealed a joint component that represented the relationship between GM volume and functional responses during the MSIT. Critically, this component

identified group differences in GM for left inferior, middle, and superior frontal cortex, left ACC, middle cingulum, left inferior parietal cortex, and right caudate associated with increased connectivity in left superior parietal cortex, left precuneus, bilateral occipital cortex as well as left middle frontal cortex. Whereas the structural feature of this component overlapped with the pattern of age-related GM differences, the functional feature comprised the network that exhibited greater connectivity (to seeds) in the old than in the young. This pattern indicates that age-related GM volume loss was associated with increased functional activation in the posterior attention network, which exhibited reliable functional connectivity to seeds (i.e. LV2) and facilitated performance in the older group. One important question regarding the joint ICA is whether the fMRI feature of a component reflects a measure of functional connectivity, given that the ICA was applied to the GLM contrast map. A recent study by Calhoun and Allen (2013) showed that the use of the feature-based ICA approach on highly distilled features (such as a GLM contrast map) yielded decompositions strikingly similar to those of the first-level ICA, which supposedly reflects functional connectivity. Thus, the fMRI feature of the jICA should reflect an indirect, but still reliable measure of functional connectivity.

Our results must be considered in light of some limitations. First, the MSIT is a general task that taxes not only cognitive interference, but also other cognitive processes such as decision-making, novelty detection, and error detection. That said, flanker interference (stimulus conflict) and Simon interference (stimulus–response conflict) are the most dominant processes in the MSIT (Stins et al., 2005), with flanker interference being larger (based on longer RT) than interference due to spatial stimulus–response incongruity (Bush et al., 2003; Stins et al., 2005). Second, a relatively small portion of the older sample failed to perform the task (5 out of 29). Although this could reflect misunderstanding of the task (two elderly subjects did not press any button at all), one cannot rule out the possibility that some older adults who failed to perform the task may not be able to successfully recruit the fronto-parietal network that promoted interference resolution in the majority of the older adults. Despite excluding outliers, there was still a considerable amount of variance within each age group. Such inter-individual variability revealed by large CIs around the correlation matrixes may partly reflect an insufficient number of subjects. Third, despite the usefulness of PLS for the purpose of the present study (e.g. extracting two networks differentially correlated with performance), it is worth nothing that the SVD approach utilized in PLS may not capture true dependencies between the patterns (McIntosh and Lobaugh, 2004). Moreover, PLS can only extract patterns of brain activity that form a linear relation with an experimental variable, behavioral measure, and/or activity from ROIs. As such, PLS ignores non-linearities in the data. In addition, the voxel-based morphometric (VBM) analysis carried out in this study has inherit limitations such as inaccuracy in spatial normalization and arbitrary choice for the size of the smoothing kernel (Bookstein, 2001). Fourth, the finding of age-related increases in functional connectivity within a fronto-parietal network may appear inconsistent with previous reports of age-related differences in functional connectivity during executive control (Clapp et al., 2011; Nagel et al., 2011; Rieckmann et al., 2012). The general pattern in these studies is that older adults show decreased fronto-parietal connectivity, but increased connectivity outside this network, particularly in contralateral prefrontal areas. However, in contrast to the aforementioned studies, we focused on trial-to-trial interference resolution with no demands on maintenance of relevant stimuli in working memory, and found increased connectivity in DLPFC and ACC to posterior regions, and decreased connectivity within the frontal cortex in aging. An interesting avenue for future research is to delineate how age-related differences in functional connectivity may depend on the specific executive control process targeted. Finally, the current findings of age-related functional reorganization were based on cross-sectional data. Past research has found marked differences in functional activation patterns in older age (e.g. increased vs. decreased brain activity) for studies using cross-sectional vs. longitudinal designs (Goh et al., 2013; Nyberg et al., 2010). For instance, a recent study by Goh and colleagues suggested that brain–behavior associations derived from cross-sectional designs (typically interpreted as a compensatory mechanism) dissociated from their longitudinal counterparts, particularly in the frontal cortex. However, another longitudinal study within the memory domain reported age-related functional reorganization consistent with our observations (Beason-Held et al., 2008). That said, future longitudinal studies are required to substantiate the observed age-related functional reorganization during interference resolution.

In summary, older adults were slower during both conditions of the MSIT. In addition, the older adults were less accurate than the young during the interference, but not the control, condition, suggesting greater susceptibility to interference in aging. The neural networks associated with accuracy differed across age. Specifically, networks with dominant contributions of anterior vs. posterior brain regions promoted good performance in younger and older adults, respectively. Structural analysis revealed age-related gray-matter losses in those anterior regions linked to good interference resolution in the young group, suggesting that the age-related functional reorganization may partly reflect structural alterations in aging.

Acknowledgments

This research was conducted at the Karolinska Institute MR-Center, Huddinge Hospital, Stockholm, Sweden. The study was supported by grants from the Swedish Research Council and Swedish Brain Power, an Alexander von Humboldt Research Award, and a donation from the af Jochnick Foundation to Lars Bäckman, and by a grant from the Swedish Research Council to Håkan Fischer. The authors wish to thank Joakim Svärd for assistance in data collection and entry, and Lars Nyberg for comments on a previous draft.

Conflict of interest

No conflict.

References

Adleman, N.E., Menon, V., Blasey, C.M., White, C.D., Warsofsky, I.S., Glover, G.H., Reiss, A.L., 2002. A developmental fMRI study of the Stroop color-word task. NeuroImage 16, 61–75.
Aron, A.R., Robbins, T.W., Poldrack, R.A., 2004. Inhibition and the right inferior frontal cortex. Trends Cogn. Sci. 8, 170–177.
Ashburner, J., 2007. A fast diffeomorphic image registration algorithm. NeuroImage 38, 95–113.
Banich, M.T., Milham, M.P., Atchley, R., Cohen, N.J., Webb, A., Wszalek, T., Kramer, A.F., Liang, Z.P., Wright, A., Shenker, J., Magin, R., 2000. fMRI studies of Stroop tasks reveal unique roles of anterior and posterior brain systems in attentional selection. J. Cogn. Neurosci. 12, 988–1000.
Beason-Held, L.L., Kraut, M.A., Resnick, S.M., 2008. I. Longitudinal changes in aging brain function. Neurobiol. Aging 29, 483–496.
Bennett, P.J., Sekuler, A.B., McIntosh, A.R., Della-Maggiore, V., 2001. The effects of aging on visual memory: evidence for functional reorganization of cortical networks. Acta Psychol. (Amst) 107, 249–273.
Bookstein, F.L., 2001. "Voxel-based morphometry" should not be used with imperfectly registered images. NeuroImage 14, 1454–1462.
Bressler, S.L., Menon, V., 2010. Large-scale brain networks in cognition: emerging methods and principles. Trends Cogn. Sci. 14, 277–290.
Buckner, R.L., Andrews-Hanna, J.R., Schacter, D.L., 2008. The brain's default network: anatomy, function, and relevance to disease. Ann. N. Y. Acad. Sci. 1124, 1–38.
Bush, G., Shin, L.M., 2006. The Multi-Source Interference Task: an fMRI task that reliably activates the cingulo-frontal-parietal cognitive/attention network. Nat. Protoc. 1, 308–313.
Bush, G., Luu, P., Posner, M.I., 2000. Cognitive and emotional influences in anterior cingulate cortex. Trends Cogn. Sci. 4, 215–222.
Bush, G., Vogt, B.A., Holmes, J., Dale, A.M., Greve, D., Jenike, M.A., Rosen, B.R., 2002. Dorsal anterior cingulate cortex: a role in reward-based decision making. Proc. Natl. Acad. Sci. U. S. A. 99, 523–528.
Bush, G., Shin, L.M., Holmes, J., Rosen, B.R., Vogt, B.A., 2003. The Multi-Source Interference Task: validation study with fMRI in individual subjects. Mol. Psychiatry 8, 60–70.
Calhoun, V.D., Allen, E., 2013. Extracting intrinsic functional networks with feature-based group independent component analysis. Psychometrika 78, 243–259.

Calhoun, V.D., Adali, T., Pearlson, G.D., Pekar, J.J., 2001. A method for making group inferences from functional MRI data using independent component analysis. Hum. Brain Mapp. 14, 140–151.
Calhoun, V.D., Adali, T., Giuliani, N.R., Pekar, J.J., Kiehl, K.A., Pearlson, G.D., 2006. Method for multimodal analysis of independent source differences in schizophrenia: combining gray matter structural and auditory oddball functional data. Hum. Brain Mapp. 27, 47–62.
Carter, C.S., Mintun, M., Cohen, J.D., 1995. Interference and facilitation effects during selective attention: an H215O PET study of Stroop task performance. NeuroImage 2, 264–272.
Clapp, W.C., Rubens, M.T., Sabharwal, J., Gazzaley, A., 2011. Deficit in switching between functional brain networks underlies the impact of multitasking on working memory in older adults. Proc. Natl. Acad. Sci. U. S. A. 108, 7212–7217.
Casey, B.J., Thomas, K.M., Welsh, T.F., Badgaiyan, R.D., Eccard, C.H., Jennings, J.R., Crone, E.A., 2000. Dissociation of response conflict, attentional selection, and expectancy with functional magnetic resonance imaging. Proc. Natl. Acad. Sci. U. S. A. 97, 8728–8733.
Corbetta, M., Shulman, G.L., 2002. Control of goal-directed and stimulus-driven attention in the brain. Nat. Rev. Neurosci. 3, 201–215.
Davis, S.W., Dennis, N.A., Daselaar, S.M., Fleck, M.S., Cabeza, R., 2008. Que PASA? The posterior–anterior shift in aging. Cereb. Cortex 18, 1201–1209.
Efron, B., Tibshirani, R., 1986. Bootstrap methods for standard errors, confidence intervals, and other measures of statistical accuracy. Stat. Sci. 1, 54–77.
Eriksen, B.A., Eriksen, C.W., 1974. Effects of noise letters upon identification of a target letter in a nonsearch task. Percept. Psychophys. 16, 143–149.
Fera, F., Weickert, T.W., Goldberg, T.E., Tessitore, A., Hariri, A., Das, S., Lee, S., Zoltick, B., Meeter, M., Myers, C.E., Gluck, M.A., Weinberger, D.R., Mattay, V.S., 2005. Neural mechanisms underlying probabilistic category learning in normal aging. J. Neurosci. 25, 11340–11348.
Folstein, M.F., Folstein, S.E., McHugh, P.R., 1975. Mini-Mental State Examination (MMSE). A practical method for grading the cognitive state of patients for the clinician. J. Psychiatr. Res. 12, 189–198.
Friston, K.J., Frith, C.D., Liddle, P.F., Frackowiak, R.S., 1993. Functional connectivity: the principal-component analysis of large (PET) data sets. J. Cereb. Blood Flow Metab. 13, 5–14.
Garavan, H., Ross, T.J., Stein, E.A., 1999. Right hemispheric dominance of inhibitory control: an event-related functional MRI study. Proc. Natl. Acad. Sci. U. S. A. 96, 8301–8306.
Gazzaley, A., Cooney, J.W., Rissman, J., D'Esposito, M., 2005. Top–down suppression deficit underlies working memory impairment in normal aging. Nat. Neurosci. 8, 1298–1300.
Gazzaley, A., Clapp, W., Kelley, J., McEvoy, K., Knight, R.T., D'Esposito, M., 2008. Age-related top–down suppression deficit in the early stages of cortical visual memory processing. Proc. Natl. Acad. Sci. U. S. A. 105, 13122–13126.
Goh, J.O., Beason-Held, L.L., An, Y., Kraut, M.A., Resnick, S.M., 2013. Frontal function and executive processing in older adults: process and region specific age-related longitudinal functional changes. NeuroImage 69, 43–50.
Good, C.D., Johnsrude, I., Ashburner, J., Henson, R.N., Friston, K.J., Frackowiak, R.S., 2001. Cerebral asymmetry and the effects of sex and handedness on brain structure: a voxel-based morphometric analysis of 465 normal adult human brains. NeuroImage 14, 685–700.
Grady, C.L., 2008. Cognitive neuroscience of aging. Ann. N. Y. Acad. Sci. 1124, 127–144.
Grady, C., 2012. The cognitive neuroscience of ageing. Nat. Rev. Neurosci. 13, 491–505.
Grady, C.L., Protzner, A.B., Kovacevic, N., Strother, S.C., Afshin-Pour, B., Wojtowicz, M., Anderson, J.A., Churchill, N., McIntosh, A.R., 2010. A multivariate analysis of age-related differences in default mode and task-positive networks across multiple cognitive domains. Cereb. Cortex 20, 1432–1447.
Gusnard, D.A., Akbudak, E., Shulman, G.L., Raichle, M.E., 2001. Medial prefrontal cortex and self-referential mental activity: relation to a default mode of brain function. Proc. Natl. Acad. Sci. U. S. A. 98, 4259–4264.
Harrison, B.J., Shaw, M., Yucel, M., Purcell, R., Brewer, W.J., Strother, S.C., Egan, G.F., Olver, J.S., Nathan, P.J., Pantelis, C., 2005. Functional connectivity during Stroop task performance. NeuroImage 24, 181–191.
Hasher, L., Zacks, R.L., 1988. Working memory, comprehension, and aging: a review and a new view. In: Bower, G.H. (Ed.), The Psychology of Learning and Motivation, vol. 2. Academic Press, San Diego, CA.
Heuninckx, S., Wenderoth, N., Swinnen, S.P., 2008. Systems neuroplasticity in the aging brain: recruiting additional neural resources for successful motor performance in elderly persons. J. Neurosci. 28, 91–99.
Hopfinger, J.B., Buonocore, M.H., Mangun, G.R., 2000. The neural mechanisms of topdown attentional control. Nat. Neurosci. 3, 284–291.
Huang, C.M., Polk, T.A., Goh, J.O., Park, D.C., 2012. Both left and right posterior parietal activations contribute to compensatory processes in normal aging. Neuropsychologia 50, 55–66.
Humberstone, M., Sawle, G.V., Clare, S., Hykin, J., Coxon, R., Bowtell, R., Macdonald, I.A., Morris, P.G., 1997. Functional magnetic resonance imaging of single motor events reveals human presupplementary motor area. Ann. Neurol. 42, 632–637.
Kalpouzos, G., Chetelat, G., Baron, J.C., Landeau, B., Mevel, K., Godeau, C., Barre, L., Constans, J.M., Viader, F., Eustache, F., Desgranges, B., 2009. Voxel-based mapping of brain gray matter volume and glucose metabolism profiles in normal aging. Neurobiol. Aging 30, 112–124.
Kalpouzos, G., Persson, J., Nyberg, L., 2011. Local brain atrophy accounts for functional activity differences in normal aging. Neurobiol. Aging 33, 623. e621–623. e613.
Krishnan, A., Williams, L.J., McIntosh, A.R., Abdi, H., 2011. Partial Least Squares (PLS) methods for neuroimaging: a tutorial and review. NeuroImage 56, 455–475.
Langenecker, S.A., Nielson, K.A., Rao, S.M., 2004. fMRI of healthy older adults during Stroop interference. NeuroImage 21, 192–200.
Lee, L., Siebner, H.R., Rowe, J.B., Rizzo, V., Rothwell, J.C., Frackowiak, R.S.J., Friston, K.J., 2003. Acute remapping within the motor system induced by low-frequency repetitive transcranial magnetic stimulation. J. Neurosci. 23, 5308–5318.
MacDonald, A.W., Cohen, J.D., Stenger, V.A., Carter, C.S., 2000. Dissociating the role of the dorsolateral prefrontal and anterior cingulate cortex in cognitive control. Science 288, 1835–1838.
Madden, D.J., Whiting, W.L., Cabeza, R., Huettel, S.A., 2004. Age-related preservation of top–down attentional guidance during visual search. Psychol. Aging 19, 304–309.
McIntosh, A.R., 1999. Mapping cognition to the brain through neural interactions. Memory 7, 523–548.
McIntosh, A.R., Lobaugh, N.J., 2004. Partial least squares analysis of neuroimaging data: applications and advances. NeuroImage 23 (Suppl. 1), S250–S263.
McIntosh, A.R., Bookstein, F.L., Haxby, J.V., Grady, C.L., 1996. Spatial pattern analysis of functional brain images using partial least squares. NeuroImage 3, 143–157.
McIntosh, A.R., Chau, W.K., Protzner, A.B., 2004. Spatiotemporal analysis of event-related fMRI data using partial least squares. NeuroImage 23, 764–775.
Milham, M.P., Erickson, K.I., Banich, M.T., Kramer, A.F., Webb, A., Wszalek, T., Cohen, N.J., 2002. Attentional control in the aging brain: insights from an fMRI study of the Stroop task. Brain Cogn. 49, 277–296.
Nagel, I.E., Preuschhof, C., Li, S.C., Nyberg, L., Backman, L., Lindenberger, U., Heekeren, H.R., 2009. Performance level modulates adult age differences in brain activation during spatial working memory. Proc. Natl. Acad. Sci. U. S. A. 106, 22552–22557.
Nagel, I.E., Preuschhof, C., Li, S.C., Nyberg, L., Backman, L., Lindenberger, U., Heekeren, H.R., 2011. Load modulation of BOLD response and connectivity predicts working memory performance in younger and older adults. J. Cogn. Neurosci. 23, 2030–2045.
Nee, D.E., Wager, T.D., Jonides, J., 2007. Interference resolution: insights from a meta-analysis of neuroimaging tasks. Cogn. Affect. Behav. Neurosci. 7, 1–17.
Nielson, K.A., Langenecker, S.A., Garavan, H., 2002. Differences in the functional neuroanatomy of inhibitory control across the adult life span. Psychol. Aging 17, 56–71.
Nyberg, L., Salami, A., Andersson, M., Eriksson, J., Kalpouzos, G., Kauppi, K., Lind, J., Pudas, S., Persson, J., Nilsson, L.-G., 2010. Longitudinal evidence for diminished frontal cortex function in aging. Proc. Natl. Acad. Sci. 107, 22682–22686.
Pascual-Leone, A., Amedi, A., Fregni, F., Merabet, L.B., 2005. The plastic human brain cortex. Annu. Rev. Neurosci. 28, 377–401.
Persson, J., Lustig, C., Nelson, J.K., Reuter-Lorenz, P.A., 2007. Age differences in deactivation: a link to cognitive control? J. Cogn. Neurosci. 19, 1021–1032.
Prakash, R.S., Erickson, K.I., Colcombe, S.J., Kim, J.S., Voss, M.W., Kramer, A.F., 2009. Age-related differences in the involvement of the prefrontal cortex in attentional control. Brain Cogn. 71, 328–335.
Prakash, R.S., Heo, S., Voss, M.W., Patterson, B., Kramer, A.F., 2012. Age-related differences in cortical recruitment and suppression: implications for cognitive performance. Behav. Brain Res. 230, 192–200.
Raichle, M.E., Snyder, A.Z., 2007. A default mode of brain function: a brief history of an evolving idea. NeuroImage 37, 1083–1090 (discussion 1097–1089).
Raichle, M.E., MacLeod, A.M., Snyder, A.Z., Powers, W.J., Gusnard, D.A., Shulman, G.L., 2001. A default mode of brain function. Proc. Natl. Acad. Sci. U. S. A. 98, 676–682.
Raz, N., Lindenberger, U., Rodrigue, K.M., Kennedy, K.M., Head, D., Williamson, A., Dahle, C., Gerstorf, D., Acker, J.D., 2005. Regional brain changes in aging healthy adults: general trends, individual differences and modifiers. Cereb. Cortex 15, 1676–1689.
Reuter-Lorenz, P.A., Lustig, C., 2005. Brain aging: reorganizing discoveries about the aging mind. Curr. Opin. Neurobiol. 15, 245–251.
Rieckmann, A., Karlsson, S., Fischer, H., Backman, L., 2012. Increased bilateral frontal connectivity during working memory in young adults under the influence of a dopamine D1 receptor antagonist. J. Neurosci. 32, 17067–17072.
Salami, A., Eriksson, J., Kompus, K., Habib, R., Kauppi, K., Nyberg, L., 2010. Characterizing the neural correlates of modality-specific and modality-independent accessibility and availability signals in memory using partial-least squares. NeuroImage 52, 686–698.
Salami, A., Eriksson, J., Nyberg, L., 2012. Opposing effects of aging on large-scale brain systems for memory encoding and cognitive control. J. Neurosci. 32, 10749–10757.
Schulte, T., Muller-Oehring, E.M., Chanraud, S., Rosenbloom, M.J., Pfefferbaum, A., Sullivan, E.V., 2009. Age-related reorganization of functional networks for successful conflict resolution: a combined functional and structural MRI study. Neurobiol. Aging 32, 2075–2090.
See, S.T., Ryan, E.B., 1995. Cognitive mediation of adult age differences in language performance. Psychol. Aging 10, 458–468.
Simon, J.R., Berbaum, K., 1990. Effect of conflicting cues on information processing: the 'Stroop effect' vs. the 'Simon effect'. Acta Psychol. (Amst) 73, 159–170.
Stern, Y., 2002. What is cognitive reserve? theory and research application of the reserve concept. J. Inter. Neuropsychol. Soc. 8, 448–460.
Stern, Y., 2009. Cognitive reserve. Neuropsychologia 47, 2015–2028.
Stevens, M.C., Skudlarski, P., Pearlson, G.D., Calhoun, V.D., 2009. Age-related cognitive gains are mediated by the effects of white matter development on brain network integration. NeuroImage 48, 738–746.
Stins, J.F., van Leeuwen, W.M., de Geus, E.J., 2005. The multi-source interference task: the effect of randomization. J. Clin. Exp. Neuropsychol. 27, 711–717.
Stroop, J.R., 1935. Studies of Interference in Serial Verbal Reactions (Reprinted from Journal Experimental-Psychology, Vol 18, Pg 643–662, 1935). J. Exp. Psychol. Gen. 18, 643–662.
Taylor, S.F., Kornblum, S., Lauber, E.J., Minoshima, S., Koeppe, R.A., 1997. Isolation of specific interference processing in the Stroop task: PET activation studies. NeuroImage 6, 81–92.
Thomsen, T., Specht, K., Rimol, L.M., Hammar, A., Nyttingnes, J., Ersland, L., Hugdahl, K., 2004. Brain localization of attentional control in different age groups by combining functional and structural MRI. NeuroImage 22, 912–919.
Tisserand, D.J., McIntosh, A.R., van der Veen, F.M., Backes, W.H., Jolles, J., 2005. Age-related reorganization of encoding networks directly influences subsequent recognition memory. Brain Res. Cogn. Brain Res. 25, 8–18.

Uttl, B., Graf, P., 1997. Color-Word Stroop test performance across the adult life span. J. Clin. Exp. Neuropsychol. 19, 405–420.
Van Dijk, K.R., Hedden, T., Venkataraman, A., Evans, K.C., Lazar, S.W., Buckner, R.L., 2010. Intrinsic functional connectivity as a tool for human connectomics: theory, properties, and optimization. J. Neurophysiol. 103, 297–321.
Verhaeghen, P., De Meersman, L., 1998. Aging and the Stroop effect: a meta-analysis. Psychol. Aging 13, 120–126.
Voss, M.W., Erickson, K.I., Chaddock, L., Prakash, R.S., Colcombe, S.J., Morris, K.S., Doerksen, S., Hu, L., McAuley, E., Kramer, A.F., 2008. Dedifferentiation in the visual cortex: an fMRI investigation of individual differences in older adults. Brain Res. 1244, 121–131.
West, R.L., 1996. An application of prefrontal cortex function theory to cognitive aging. Psychol. Bull. 120, 272–292.
Williams, Z.M., Bush, G., Rauch, S.L., Cosgrove, G.R., Eskandar, E.N., 2004. Human anterior cingulate neurons and the integration of monetary reward with motor responses. Nat. Neurosci. 7, 1370–1375.
Zarahn, E., Rakitin, B., Abela, D., Flynn, J., Stern, Y., 2007. Age-related changes in brain activation during a delayed item recognition task. Neurobiol. Aging 28, 784–798.
Zysset, S., Schroeter, M.L., Neumann, J., von Cramon, D.Y., 2007. Stroop interference, hemodynamic response and aging: an event-related fMRI study. Neurobiol. Aging 28, 937–946.